EduHeart Book Publishing
Asian Research Journal of Education, 2024
E-ISSN: 3028-0842
P-ISSN: 3028-0834
Vol. 1 Issue 1

Dynamic Path Planning Method for Flat-Land Fancy Roller Skating Based on Multi-Sensor Information Fusion

Meng, Xianlu
https://orcid.org/0009-0002-4640-8231
University of the East
meng.xianlu@ue.edu.ph

ABSTRACT

With the improvement of sports enthusiasts' competitive level, the path planning of flat-land fancy roller skating has become a concern for people. This research mainly discusses the method of dynamic path planning for flat fancy roller skating based on multi-sensor information fusion. This research first uses the particle swarm algorithm to search for the global optimal path, and then uses the ant colony algorithm to perform a second search on the optimal path obtained by the particle swarm algorithm to obtain the optimal solution. Applying voltage stimulates the transducer to emit ultrasonic waves in pulse form, after which it transitions into a receiving state to analyze the received ultrasonic waves. Once the inspection confirms that the signal it detected is the echo of the emitted ultrasonic wave, it calculates the distance between the measured obstacle and the sensor using the transit time principle. The mobile pulley can measure the coordinate information of the mobile pulley in the global environment through the positioning measuring instrument and then compare it with the previously planned path to determine the position deviation of the mobile pulley. In order to improve the real-time performance and reliability of the system, the data collection and data fusion of the sensors are realized by a two-level distributed system. The ultrasonic sensor and its control interface board adopt the single-chip microcomputer control system produced by the American HelpMate Company. The ultrasonic transducer is both a transmitter and a receiver. The maximum measuring distance of the ultrasonic sensor can be programmed to be 0.1m-10m. The robust performance index (ER) is very different before and after the improvement. The improved algorithm is only 0.87%, which is far less than 8.12% in the basic ant colony algorithm. In the case of the same number of iterations, the path length of the improved algorithm is longer than that of the basic algorithm. This research will greatly enhance the superiority of dynamic path planning for flat-land fancy roller skating.

Keywords: *Multi-sensor information fusion, flat-land fancy roller skating, dynamic path planning, ant colony algorithm, ultrasonic sensor*

INTRODUCTION

In recent years, flat-land fancy roller skating has been sought after by contemporary college students for its unique fitness value and sports connotation. Compared with other sports, roller skating has lower requirements on weather, venue, and other conditions, as well as lower requirements on the physical fitness of the practitioners. Fancy roller skating on flat ground is highly ornamental, interesting, and entertaining, and it has a strong promotion effect on improving body functions.

As a new sport, flat-land fancy roller skating has the embodiment of goodness and beauty pursued by the new human beings bred in the new era. Multi-sensor information fusion technology can comprehensively process various types of information and effectively improve the reliability and accuracy of that information. Therefore, the research on the path planning of fancy roller skating on flat ground based on multi-sensor information fusion is of great significance and application value.

The wireless sensor network (WSN) has attracted the research interest of a large number of scholars, especially in the context of performing surveillance and surveillance tasks. The purpose of F. Caron is to develop a GPS/IMU multi-sensor fusion algorithm. He uses contextual information to detect and reject bad data transmitted by GPS sensors, thereby improving reliability. He directly provides the acceleration provided by the IMU based on the fusion process of the multi-sensor Kalman filter. Although the filter developed here can easily add other sensors to achieve the required performance, the research lacks innovation. Yang X's research involves multi-rate distributed fusion estimation of maneuvering target tracking in wireless sensor networks (WSN). In consideration of energy efficiency and tracking accuracy, he proposed a multi-rate fusion strategy and a hierarchical, two-level fusion structure. In the first stage, a locally improved strong tracking filter estimator is designed to obtain a local estimate of each cluster head in the WSN. In the second stage, a multi-rate fusion estimator is designed to generate a fusion estimate with higher estimation accuracy. Although the fusion estimation method in his research can provide satisfactory estimation accuracy while reducing the sampling rate and estimation rate, the research still lacks data. Jin H believes that demonstration-based control is an effective method to improve execution stability in some complex desktop object operation tasks of the robot system. He used a new optical hand tracking sensor called Leap Motion to perform non-contact demonstrations of the robotic system. At the same time, he developed the coordinate system of the Mult-Leap Motion hand-tracking device and the robot demonstration system. Although he conducted gesture recognition and scene experiments, the multi-leap motion hand-tracking system he proposed lacked improvement in the desktop object operation tasks demonstrated by the robot. Fei Z believes that it is challenging to make compelling compromises between various conflicting optimization standards. He provides tutorials and surveys of the latest research and development work using multi-objective optimization (MOO) techniques to solve this problem. First, he outlines the main optimization goals used in WSN. He then elaborated on various popular methods envisaged for MOO. Although he summarized a series of recent studies on MOO in the context of WSN, the research lacks innovative awareness.

This research first uses the particle swarm algorithm to search for the global optimal path and then uses the ant colony algorithm to perform a second search on the optimal path obtained by the particle swarm algorithm to obtain the optimal solution. When it is confirmed that the signal detected by the inspection is the echo of the emitted ultrasonic wave, the distance between the measured obstacle and the sensor is calculated according to the principle of transit time. The mobile pulley can measure the coordinate information of the mobile pulley in the global environment through the positioning measuring instrument and then compare it with the previously planned path to determine the position deviation of the mobile pulley. To improve the real-time performance and reliability of the system, the data collection and data fusion of the sensors are realized by a two-level distributed system.

METHODOLOGY

Research Design

This study utilizes a thorough methodology to create and assess a dynamic path planning technique for flat-land fancy roller skating by utilizing the fusion of multi-sensor information. The methodology combines sophisticated computational methods with real-world sensor data to improve the accuracy and efficiency of path planning.

Algorithm Development

The initial phase of the process entails the creation of two fundamental algorithms: Particle Swarm Optimization (PSO) and Ant Colony Optimization (ACO). The PSO method is employed to systematically search the solution space and determine the most optimal path for the roller skate trajectory across the entire global space. This process entails the initialization of a group of potential solutions (particles) and the subsequent iterative adjustment of their placements, taking into account both individual and collective experiences, in order to discover the most effective path. The search method is guided by defining key parameters, such as particle velocity and location limitations. After the Particle Swarm Optimization (PSO) process, the Ant Colony Optimization (ACO) method is used to conduct a supplementary search on the path that was determined by the PSO. The ACO algorithm emulates the actions of ants to enhance the path by releasing pheromones and repeating the process until the best solution is obtained. The algorithm's performance is improved by adjusting parameters such as the rate at which pheromones evaporate and the size of the colony.

Sensor Integration

Ultrasonic sensors are crucial for measuring the distances between the skate route and obstacles, in addition to the construction of algorithms. Ultrasonic waves are emitted through voltage stimulation, and the time it takes for the echo to return is evaluated in order to determine the distances of obstacles. The ultrasonic sensors, under the direction of a single-chip microcontroller, are designed to measure distances ranging from 0.1m to 10m. In addition, a mobile pulley positioning system is used to monitor the coordinate data of the mobile pulley in the global environment. The system compares real-time data with the intended path to evaluate any differences in position.

Data Collection and Fusion

Data gathering and fusion are essential aspects of this research. Data from sensors, such as ultrasonic sensors and the mobile pulley positioning system, are gathered in a controlled skating environment on flat terrain. To enhance real-time performance and dependability, a distributed system with two levels is employed to integrate and process the data. Data fusion, accomplished using sophisticated methods, improves accuracy and minimizes noise by combining information from many sensors.

Performance Evaluation

In order to assess the efficacy of the suggested approach, performance measurements such as the Robust Performance Index (ER) and path length comparison are employed. Prior to and following algorithm enhancements, the ER is examined to evaluate its resilience, while the improved algorithm's path length is compared to that of the fundamental ant colony method.

The system's performance is validated using simulations and real-world experiments, with a specific focus on its real-time path adjustment and obstacle avoidance capabilities.

Ultimately, the research findings are examined and documented. The documentation contains an assessment of the algorithm's efficiency, the efficacy of sensor integration, and the general reliability of the system. The significance of the results for dynamic path planning in flat-land fancy roller skating are reviewed, and suggestions for future research and development are given.

Fancy Roller Skating Dynamic Path Planning on Flat Ground

Multi-Sensor Information Fusion

In a multi-sensor network, each sensor is called a local node, and the target tracked by each sensor is called local tracking, and the tracking target after fusion is called global tracking. The multi-sensor target association is performed, and then global tracking is obtained through fusion calculation, which realizes the update of the fusion target and obtains a new and higher-precision fusion result. The two commonly used methods of intelligent pulley fusion are measurement fusion and state vector fusion. Normally, the measurement fusion method is the best, but the calculation efficiency is low; the state vector fusion algorithm is more efficient, but the result is suboptimal. Measurement fusion and state vector fusion correspond to the centralized and distributed fusion frameworks, respectively. The linear system is used when deriving the commonly used methods of measurement fusion and state vector fusion, and the conclusion can be extended to nonlinear systems. Multi-sensor state estimation is shown in Figure 1.

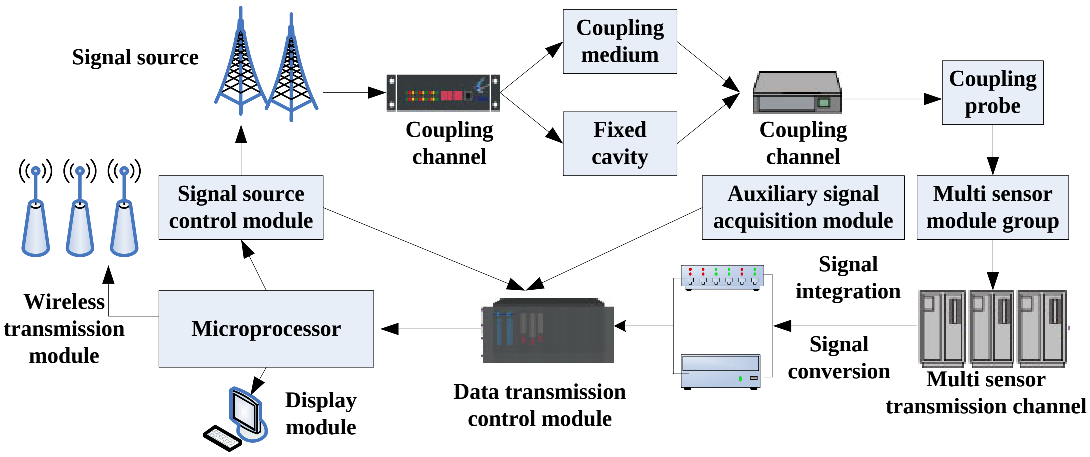

Figure 1. Multi-sensor state estimation

Assuming the same target of target a in sensor g and target b in sensor h, that is, $x_a(k) = x_b(k)$, the state estimation error is:

$$\tilde{x}_a^g(k) = x_a(k) - \hat{x}_a^g(k)$$

$$\tilde{x}_b^g(k) = x_b(k) - \hat{x}_b^g(k)$$

$\tilde{x}_a^g(k)$ and $\tilde{x}_b^g(k)$

are independent of each other, then the covariance of the difference in target state estimates between sensors is:

$$C_{ab}(k) = E\left(d_{ab}(k)d_{ab}(k)^T\right) = E\left[\left(\hat{x}_a^g(k) - \hat{x}_h^g(k)\right)\left(\hat{x}_a^g(k) - \hat{x}_h^g(k)\right)^T\right] = P_a^g(k) + P_b^h(k)$$

Among them $P_a^g(k)$ is the estimated error covariance of target a in sensor g, and $P_b^h(k)$ is the error covariance of target b in sensor h. At time k, the normalized difference of the state vectors of target a in sensor g and target b in sensor h is:

$$u_{ab}(k) = \frac{d_{ab}}{\sqrt{C_{ab}(k)}}$$

Among them, $d_{ab}(k) = \hat{x}_a^g(k) - \hat{x}_h^g(k)$, $C_{ab}(k) = P_a^g(k) + P_b^h(k)$.

Since the sensor has a certain sampling period, it is necessary to discretize the Gaussian white noise:

$$n_d[k] = n(t_0 + \Delta t) \approx \frac{1}{\Delta t}\int_{t_0}^{t_0+\Delta t} n(\tau)d\tau$$

$$E(n_d[k]^2) = E\left(\frac{1}{\Delta t^2}\int_{t_0}^{t_0+\Delta t}\int_{t_0}^{t_0+\Delta t} n(\tau)n(t)d\tau dt\right) = E(\frac{\sigma^2}{\Delta t})$$

That is, $n_d[k] = \sigma_d w[k]$, where $\sigma_d = \sigma\frac{1}{\sqrt{\Delta t}}$.

By studying the static and dynamic performance of different sensors, different sensor data can be obtained with different frequency domain characteristics. According to whether the sensor signal contains high-frequency noise or low-frequency noise, select a specific filter in the complementary filter to remove the corresponding noise, and finally add multiple filtered signals to obtain an effective signal of the entire frequency band, completing the entire denoising and fusion process. Assuming that the attitude detection system contains two sensors, their output values contain low-frequency noise and high-frequency noise, respectively, and the attitudes in the frequency domain obtained from them are $C_1(s)$ and $C_2(s)$ respectively. If the real attitude is $C(s)$ there is the relationship is as follows:

$$\begin{cases} C_1(s) = C(s) + \mu_L(s) \\ C_2(s) = C(s) + \mu_H(s) \end{cases}$$

The state equation of the moving target in the Cartesian coordinate system is:

$$x(k+1) = F(k)x(k) + \Gamma(k)v(k)$$

In the formula, $x(k) \in R^{n\times 1}$ is the target state vector at time k.

Fancy Roller Skating on Flat Ground

In the new fashion movement achieved by this rapidly developing society, people are more yearning to get rid of the mask of hypocrisy in real life, to find a truer self in flat-land fancy roller skating, and to pursue a more active and healthy spiritual world. Roller skating not only has the ability to improve and develop a person's agility, strength, balance, speed, flexibility, endurance, and coordination; moreover, roller skating can also improve the function of the human body's internal organs. It can improve the blood circulation system and increase human breathing. The system has a good effect; at the same time, roller skating can also exercise people's will and quality and cultivate people's ability to make positive and decisive judgments.

Because flat-land fancy roller skating and speed roller skating belong to the sub-projects of roller skating, they have a lot in common. To learn flat-land fancy roller skating, you must also master the basic skills of roller skating, such as standing, sliding, cornering, emergency stopping and other skills. A flat-skating enthusiast who does not have any basic skating foundation will encounter greater obstacles in improving the speed and range of flat-skating technology compared to a basic enthusiast. Therefore, as a college physical education teacher, you can fully base your career on your own special job position, use your rich professional knowledge and superb professional skills, and provide useful guidance to flat-land fancy roller skating enthusiasts, and for the emerging of flat-land fancy roller skating. The sport can make a greater contribution to the better development of ordinary colleges and universities.

Dynamic Path Planning

The pheromone concentration on the road section is constantly volatile, so when the road section is constantly selected by ants, the pheromone concentration on the road section will be continuously strengthened, and the road section will be more likely to be selected by other ants behind it. Other road sections become longer, and the pheromone gradually evaporates. The probability of this road section being selected by ants gradually decreases, and the probability of being abandoned increases. After a period of time, the optimal path will be completely found. Of course, if the ants encounter a new intersection and there is no path that has been selected, they randomly choose one of the paths and leave the information related to the path as a reference for the ants behind them. Through such pheromone transmission, the ant colony algorithm has a positive feedback mechanism. For this reason, the obstacle avoidance strategy was adopted at the early stage of the search, and the obstacle avoidance factor $safety_j$ was added as:

$$p_{ij}^k(t)=\begin{cases}\dfrac{[\tau_{ij}(t)]^{\alpha}[n_{ij}(t)]^{\beta}[safety_j]^{\varepsilon}}{\sum_{j\in allow_k}[\tau_{ij}(t)]^{\alpha}[n_{ij}(t)]^{\beta}[safety_j]^{\varepsilon}}, & j\in allow_k\\ 0, & j\notin allow_k\end{cases}$$

$$safety_j=\frac{A_j-O_j-L_j}{A_j}$$

Where O_j is the total number of grids adjacent to node j and there are obstacles? L_j refers to the total number of grids adjacent to node j and restricted by the taboo table. Adopt parameter-adaptive pseudo-random transfer strategy:

$$j = \begin{cases} \arg\max\left([\tau_{ij}(t)]^{\alpha}[n_{ij}(t)]^{\beta}[safety_j]^{\varepsilon}\right), q \le q0 \\ p_{ij}^{k}, else \end{cases}$$

$$q0 = \delta \frac{N_{\max} - N_m}{N_{\max}}$$

Where $N_{\max}$ is the maximum number of iterations, and N_m is the current number of iterations. In the iterative process, t is the time scale. The ant takes one step forward. The algorithm is iterated once, and the pheromone is updated once. The update of the pheromone is manifested as the increase and volatilization of the pheromone. The pheromone update formula is as follows:

$$t_{ij}(t+1) = (1-r)t_{ij}(t) + t_{ij}(t)$$

Among them, the value of the volatilization coefficient $\rho \subset [0,1)$, $(1-\rho)$ indicates the pheromone remaining on the path after volatilization and $\Delta\tau_{ij}(t)$ indicates that when all ants have selected the next path, all the choices in the previous step of the ant movement are from i to j. The sum of the pheromone left by the ants on the path, the initial value $\Delta\tau_{ij}(0) = 0$, the expression is:

$$\Delta\tau_{ij}(t) = \sum_{k=1}^{m} \tau_{ij}^{k}(t)$$

In the formula, $\tau_{ij}^{k}(t)$ represents the pheromone left by the k-th ant on the path ij at time t.

Experiment with Dynamic Path Planning for Fancy Roller Skating on Flat Ground

Ant-Colony Algorithm

Aiming at the shortcomings of the ant colony algorithm, this paper proposes a particle colony ant colony fusion algorithm that combines particle swarm optimization and an improved ant colony algorithm. First, the particle swarm algorithm is used to perform a rough search on the global path, and the dynamic intelligent distribution of pheromone is carried out while searching. The initial distribution of pheromones in the ant colony algorithm is obtained, and some poor paths are eliminated according to the pheromone content. Then use the ant colony algorithm to perform a second search on the optimal path obtained by the particle swarm algorithm, and finally obtain the optimal solution.

Mobile Pulley Environment Perception System

This system uses 8 ultrasonic sensors to detect obstacles in the surrounding environment of the moving pulley. The ultrasonic transducer is a disc-shape device with a diameter of 3.6 cm that is both a transmitter and a receiver. When it is confirmed that the signal detected by the inspection is the echo of the emitted ultrasonic wave, the distance between the measured obstacle and the sensor is calculated according to the principle of transit time.

In order to shorten the time, it takes for 8 ultrasonic sensors to detect one week in a loop and to minimize cross-interference, the 8 sensors can be divided into two groups according to the orthogonal position relationship, and 4 sensors in a group are activated at the same time each time. The state (start or stop) of the ultrasonic sensor and the maximum measurement distance can be set online through software programming.

In this system, the grid size is 10cm×10cm. Each grid has a credibility value CV (Certainty Value), which is used to indicate the credibility of obstacles in the area. This value is updated by a probability function that takes into account the uncertainty of the ultrasonic sensor.

The mobile pulley can measure the coordinate information of the mobile pulley in the global environment through the positioning measuring instrument and then compare it with the previously planned path to determine the position deviation of the mobile pulley. Through the calculation of the fuzzy control module, the position and angle of the moving pulley that need to be compensated are solved and then allocated to the four drive units, that is, the four motors. According to the previously calculated kinematics model of the moving pulley, the speed of each wheel is calculated and finally reached. The role of adjusting the posture of the moving pulley.

Distributed Multi-Sensor System Structure

In order to improve the real-time performance and reliability of the system, the data collection and data fusion of the sensors are realized by a two-level distributed system. The low level of the system consists of independent data acquisition subsystems for the three types of sensors. Among them, the control and data detection of the laser sensor are completed by a self-developed 89C51 single-chip microcomputer system. The ultrasonic sensor and its control interface board adopt the single-chip microcomputer control system produced by the American HelpMate Company. The ultrasonic transducer is a disc-shape device with a diameter of 3.6cm, which is both a transmitter and a receiver. The maximum measuring distance of the ultrasonic sensor can be programmed to be 0.1m-10m. For the odometer sensor, an industrial computer responsible for path planning and motion control completes data collection and positioning calculations. The data fusion computer communicates with the above three sensor subsystems through serial port 1, serial port 2, and a parallel port to exchange data.

The sampling period T of data fusion is 200 ms. In each period, the data fusion computer needs to complete the following operations:

(1) Read the road marking data from the laser sensor. If the number of matched road signs is greater than 3, the pose of the moving pulley is calculated according to the positioning algorithm. Otherwise, the posture of the moving pulley is determined using the odometer sensor data (update this data through the interrupt service program);

(2) Read in the data from the ultrasonic sensor and update the grid map;

(3) Use advanced data fusion methods to obtain various environmental characteristics;

(4) Transmit various environmental characteristics to the path planning and motion control computers;

(5) Adjust the ultrasonic sensor scheduling strategy according to the posture of the moving pulley and environmental characteristics.

3.4 Combination of Slip Compensation Control and Adaptive Sliding Mode Control (Sliding Mode Control, SMC)

By controlling the rotation speed of the virtual pulleys on both sides, the motion control of the skater's motion center can be realized, so that the skater can plan the movement of the path as desired.

In addition, if the virtual pulleys on both sides slip and the slip rate is not coordinated, it will also cause the difficulty of passing through the planned path route area to exceed the movement ability of the moving pulley. If the local is extremely small, the pulley may appear. Slippage phenomenon, which can be achieved by a proper path planning method for the slip of the pulley and the body. These complex slip situations are difficult to calculate or predict in real time, but the time-varying longitudinal slip rate of the pulley can be directly obtained by kinematic analysis of the virtual pulleys on both sides, which is convenient to solve. Therefore, the influence of longitudinal slip on the movement is mainly considered.

When applying the designed method to the trajectory tracking control system of the pulley, it is necessary to use the slip compensation controller as the feedforward controller and the adaptive SMC controller as the main control loop. The adaptive SMC controller first obtains the ideal output of the current system according to the deviation of the expected and actual motion states at the last moment. The slip compensation feedforward controller compensates the ideal output according to the longitudinal slip rate information calculated in real time. After the motion actuator of the moving pulley runs according to the instructions for compensation, the mileage measurement mechanism collects the actual motion state and continues the above cycle.

3.5 Multi-Sensor Data Fusion Model

This study uses the multi-level data fusion model shown in Figure 2. First of all, the roller skates start from a known position. The sampling period of the laser absolute positioning sensor is 200ms, and the sampling period of the internal odometer is 10ms. Calculate to estimate the position and posture of roller skates, and the data of the absolute sensor can periodically correct the cumulative error of the internal sensor. The positioning research using this algorithm has strong robustness. Then, according to the position and posture of the roller skates and the data measured by the ultrasonic sensor, the location range of the obstacle on the environment map represented by the grid is determined. Finally, on the basis of the grid map, advanced data fusion methods (such as the method of identifying obstacle groups) are used to extract environmental features for path planning, mission planning, etc. The dotted line from the research point to the node represents the signal that the integrated function program under research may send to the node. Figure 2 lists three typical functions in the data fusion process. "Sensor selection" can complete the optimal management of multiple sensors, such as selecting and starting a suitable ultrasonic sensor to detect obstacles in the forward direction for changes in the direction of movement and determining the maximum detection range of the ultrasonic sensor according to the known obstacle distribution according to road signs. The detection result determines whether to apply laser sensor positioning and so on. The information of ultrasonic sensors can be stored in the "environmental model," and the information of different sensors needs to be "data conversion" of coordinates or data units before being fused to achieve a unified knowledge representation. At first, the original data from the sensor existed in the form of signals. After a series of data fusions, the signals will be further converted into more abstract digital or symbolic representations.

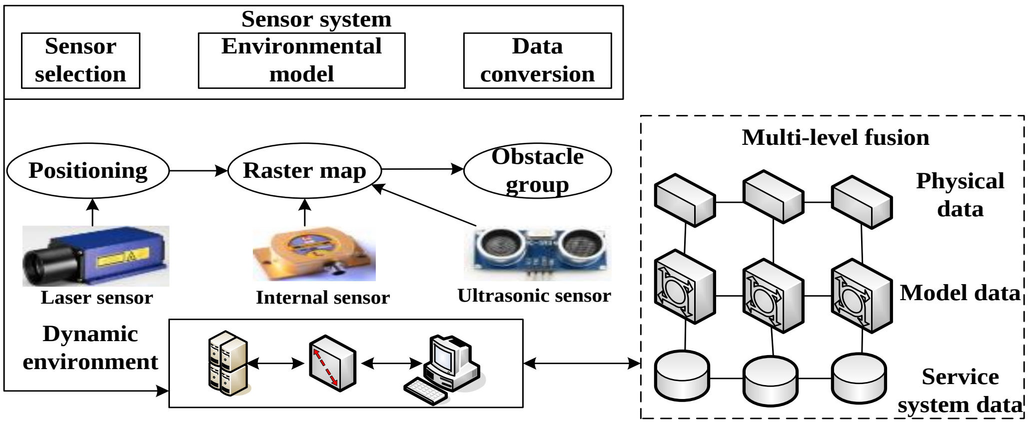

Figure 2. Multi-level Data Fusion Model

RESULTS AND DISCUSSION

The parameter ρ in the ant colony model represents the pheromone volatilization coefficient. The value of pheromone ρ is related to the volatilization speed of the pheromone and has an extremely important impact on the convergence speed of the algorithm and the global search performance. 1-ρ represents the pheromone residual coefficient, which represents the remaining pheromone on the node. When the value of ρ is large, the probability that the path node that has been searched will be selected again is also greater, which will greatly interfere with the search randomness and globality of the algorithm; on the contrary, when the value of ρ is small, the pheromone volatilize speed is slow, and the chance of new ants choosing a path that has not been selected before has increased, which can improve the randomness and global ability of the algorithm, but the convergence speed of the algorithm will correspondingly decrease. The impact of the ant colony algorithm on the environment is shown in Table 1.

Table 1.

The impact of ant colony algorithm on the environment

Volatility coefficient ρ	Average optimal solution	Average number of iterations	Operation hours
0.1	33.2739	Divergence	8.0s
0.2	30.1881	47	7.8s
0.4	28.6274	42	7.4s
0.6	28.6274	29	7.4s
0.8	29.1274	22	6.8s

If you want to achieve the optimal convergence speed and optimal path at the same time, when other parameters are the same, the pheromone volatilization coefficient has a great influence on the overall performance of the algorithm. ρ is approximately in an inverse relationship with the number of iterations of the algorithm. In the range of 0.1-0.9, the larger the p, the smaller the number of iterations. This is because when ρ is small, the pheromone gap on the node is not big, the random performance of the search is strengthened, the pheromone in the grid can be kept for a long time, and the result of the solution is not strong in the feedback information of the problem, so the search speed is relatively slow; when ρ is large, the core position of the algorithm is the positive feedback of information. Although the iterative convergence speed is accelerated, the result is easy to fall into the local optimum. The impact of the improved ant colony algorithm on the environment is shown in Table 2.

Table 2.

The impact of improved ant colony algorithm on the environment

Volatility coefficient ρ	Average optimal solution	Average number of iterations	Operation hours
0.1	33.4558	Divergence	7.0s
0.2	31.5465	48	6.1s
0.4	27.4558	34	8.2s
0.6	27.4558	22	6.3s

0.8	27.4558	13	5.6s

The performance of the algorithm in different situations is shown in Figure 3. It can be seen from Figure 3 that when ρ≤0.2, the algorithm converges slowly, and it is difficult to obtain a fixed solution for convergence; when ρ≥0.8, the algorithm falls into a local minimum. When the value of ρ is about 0.5, the overall performance of the algorithm is the best, the convergence speed and global performance of the algorithm are better, and the calculation performance is relatively stable.

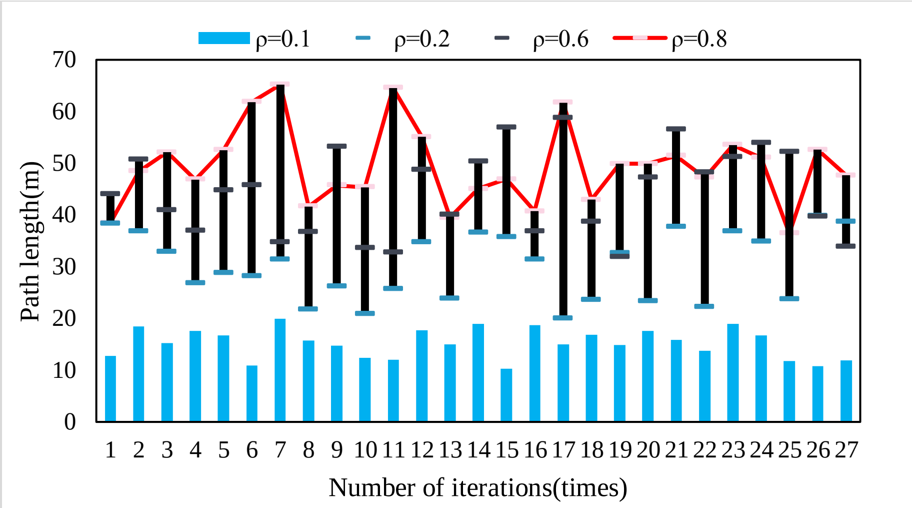

Figure 3. Performance of the algorithm in different situations

A series of simulations were designed to investigate the influence of whether to perform slip compensation and whether to apply adaptive parameter adjustment to the SMC controller on the tracking effect of the pulley trajectory. The CPU model of the simulation platform is Intel@G4600. All units in the simulation are SI. Figure 4 shows the comparison of simulation results for the circular trajectory tracking position with or without slip compensation.

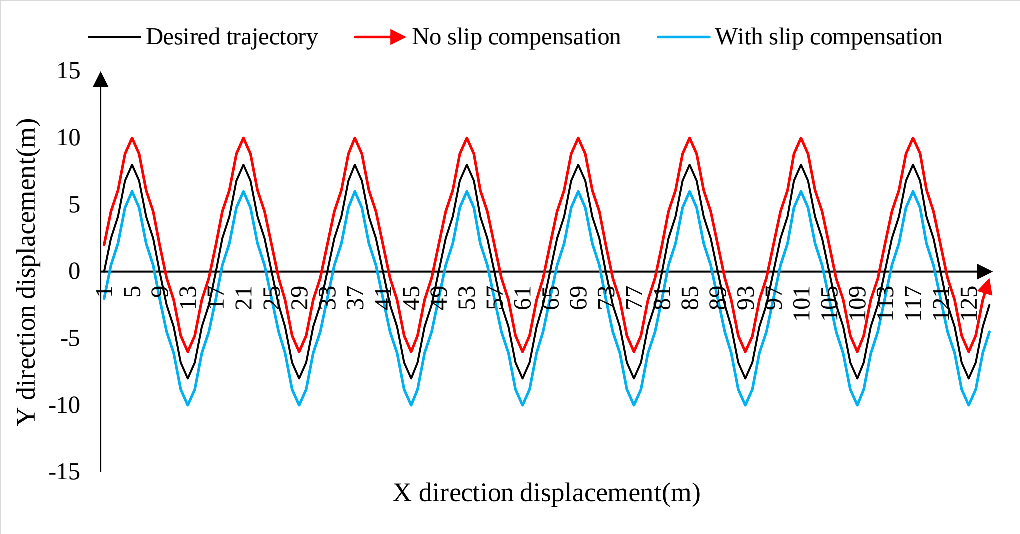

Figure 4. Comparison of simulation results of circular trajectory tracking positions with or without slip compensation

The actual line speed comparison is shown in Figure 5. It can be clearly seen that for the time-varying slip rate, if slip compensation is not applied, ordinary SMC alone cannot achieve a better trajectory tracking effect.

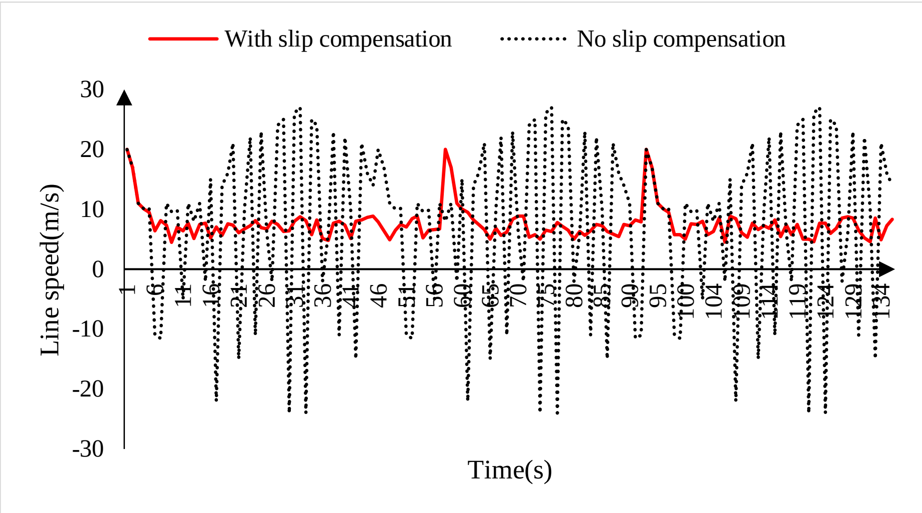

Figure 5. Actual line speed comparison

The actual angular velocity comparison is shown in Figure 6. It can be clearly seen from the comparison figure that if slip compensation is not applied, the actual trajectory will be affected by the time-varying slip rate and there will be severe chattering. When slip compensation is applied, the result of trajectory tracking is relatively smooth, almost not affected by the time-varying slip rate.

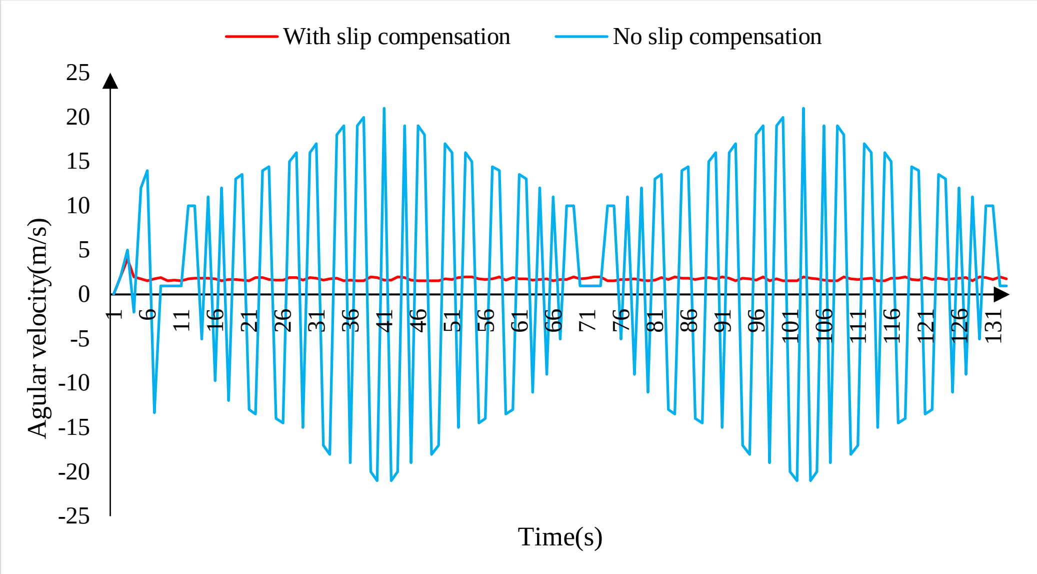

Figure 6. Actual angular velocity comparison

Through the comparative analysis of the experimental results, it can be seen that in the experiments carried out, the improved ant colony algorithm and the basic ant colony algorithm can obtain the best known solution, but the worst solution obtained by the two algorithms is very different, and the improved algorithm is obvious. It is better than the basic ant colony algorithm, which shows that the improved algorithm has better global search capabilities and that the solution results are more stable and of higher quality. The processing comparison of the algorithm is shown in Table 3.

Table 3.

Algorithm processing comparison

Algorithm	Optimal solution	Worst solution	Number of iterations
Basic algorithm	28.6274	33.2739	42
Improve algorithm	28.6274	29.1274	21

Although the best performance index E0 is the same and both are 0, the robust performance index ER is very different before and after the improvement. The improved algorithm is only 0.87%, which is much smaller than the 8.12% in the basic ant colony algorithm, and the number of iterations is the same. The algorithm's robust performance comparison is shown in Table 4.

Table 4.

Comparison of algorithm robust performance

Algorithm	E0	ER
Basic algorithm	0	8.12%
Improve algorithm	0	0.87%

Further data statistics are carried out on the accumulation of errors, and the percentage of the cumulative value of the absolute error and the expected change value of the actual trajectory are calculated. This data reflects the instantaneous response capability of trajectory tracking. If the cumulative value of the absolute error is higher, the instantaneous response capability is indicated. The worse. The statistical results are shown in Table 5. It can be seen from the above comparison that after applying slip compensation, the cumulative value of the displacement error in the X direction increases and the cumulative error value in the Y direction and steering angle decreases; that is, the response speed is relatively fast. In general, the application of slip compensation can improve the response speed of the moving pulley to the target trajectory when the time-varying slip rate exists to a certain extent. A more significant improvement is to reduce the output shock of the control system caused by the slip so that the trajectory can be tracked. The process is smoother and controllable. In summary, slip compensation significantly improves the working ability of the trajectory tracking system.

Table 5.

Statistical results

Program	X direction displacement	Y direction displacement	Steering angle
No slip compensation	18.538%	10.1 59%	10.911%
Apply slip compensation	24.428%	1.1 9%	4.951%

Figure 7 shows the comparison of simulation results for the cosine trajectory tracking position of the SMC method with adaptive control or not. It can be seen that, in the first turn, the trajectory position, linear velocity and angular velocity of the adaptive SMC have a large chattering. This is caused by the lack of robustness of the system during the start-up process of the adaptive adjustment. However, in all subsequent turns, the trajectory position, linear velocity, and angular velocity of the adaptive SMC are smoother than those of the ordinary SMC, and there is almost no obvious jitter.

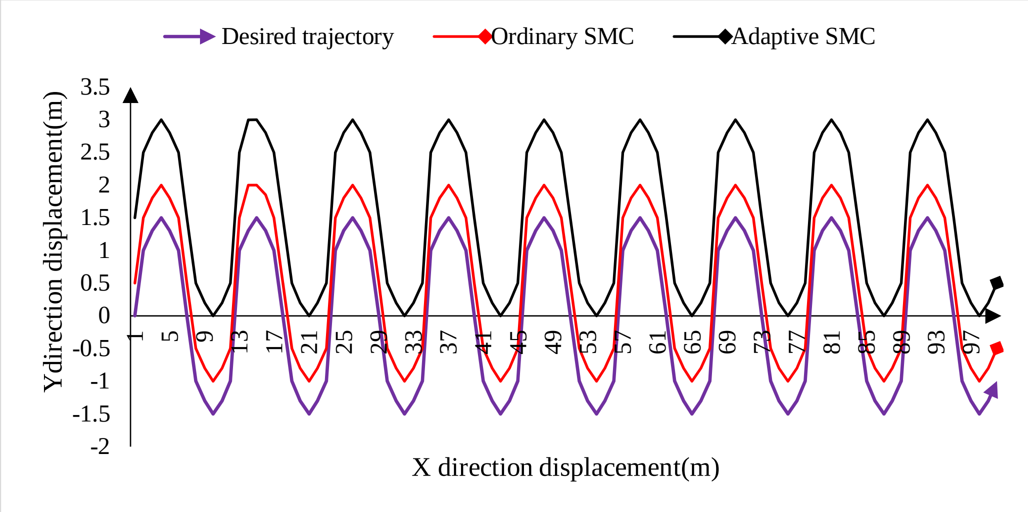

Figure 7. Comparison of simulation results of the cosine trajectory tracking position of the SMC method with adaptive control or not

The numerical change of the adaptive function is shown in Figure 8. It can be seen that the system adjusts the parameters adaptively as the movement changes. It can be clearly seen from the comparison chart that in the first turn, the system has a large error due to the effect of adaptive parameter adjustment, but the normal SMC still oscillates at all subsequent turns, and adaptive SMC has almost no obvious oscillations.

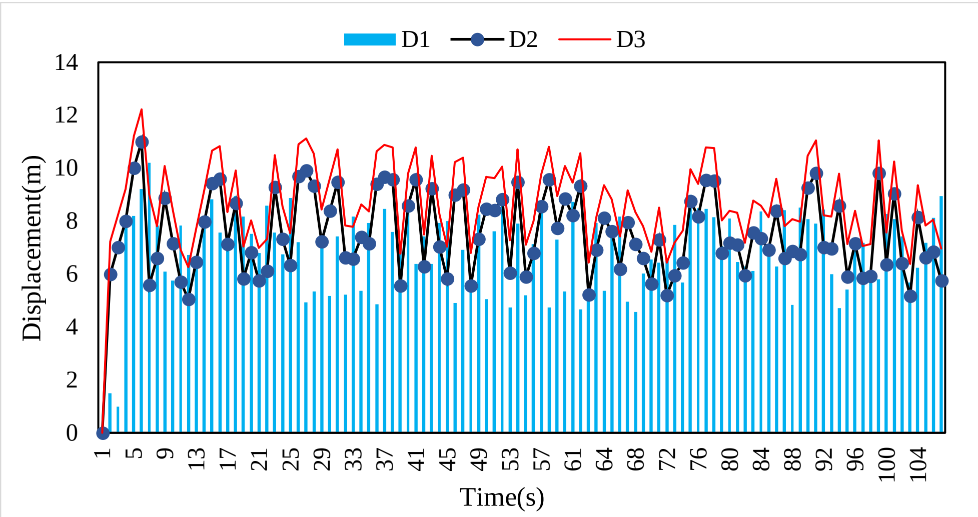

Figure 8. The numerical change of the adaptive function

The above comparison results show that the ordinary SMC is suitable for trajectory tracking tasks that focus on transient responses, while the adaptive SMC is suitable for situations where the working time is long enough and the process of tracking the trajectory is not expected to have more chattering. In practical applications, since the chattering of the system will bring greater uncertainty to the tracking of the trajectory, the adaptive SMC has a good suppression effect on the output chattering due to the basic adaptation of the parameter adjustment, which can be better for the system. In summary, both slip compensation and adaptive SMC control can greatly reduce the chattering of the system output and can largely suppress the system operation deviation caused by the slip rate change and the input information change. In actual applications, this effect of suppressing system output chattering is conducive to enhancing WMR trajectory tracking. The absolute error-cumulative value comparison is shown in Table 6.

Table 6.

Absolute error cumulative value comparison

SMC	**Displacement in X direction**	**Y direction displacement**	**Steering angle**
Ordinary SMC with slip compensation	2.35%	23.866%	342.2 5%
Adaptive SMC with slip compensation	2.524%	24.387%	342.07%

CONCLUSION

This research first uses the particle swarm algorithm to search for the global optimal path, and then uses the ant colony algorithm to perform a second search on the optimal path obtained by the particle swarm algorithm to obtain the optimal solution. When voltage is applied, the transducer is stimulated to emit ultrasonic waves in pulse form, and then the transducer turns into the receiving state to analyze the received ultrasonic waves. When it is confirmed that the signal detected by the inspection is the echo of the emitted ultrasonic wave, the distance between the measured obstacle and the sensor is calculated according to the principle of transit time. The mobile pulley can measure the coordinate information of the mobile pulley in the global environment through the positioning measuring instrument and then compare it with the previously planned path to determine the position deviation of the mobile pulley. In order to improve the real-time performance and reliability of the system. This research will greatly enhance the superiority of dynamic path planning process for flat-land fancy roller skating. In the entire path planning, roller skating is regarded as a point. Future research needs to take the size, and shape of the roller skate into account, further optimize and improve the improved algorithm, and apply it to the actual situation.

REFERENCES

A, H., A, A. B. R., G, T. O. A. F., & et al. (2018). Physical assessment of coastal vulnerability under enhanced land subsidence in Semarang, Indonesia, using multi-sensor satellite data. Advances in Space Research, 61(8), 2159-2179. https://doi.org/10.1016/j.asr.2018.02.007

Barbosh, M., Sadhu, A., & Vogrig, M. (2018). Multisensor-based hybrid empirical mode decomposition method towards system identification of structures. Structural Control and Health Monitoring, 25(5), e2147.1-e2147.21. https://doi.org/10.1002/stc.2147

Bhardwaj, J., Gupta, K. K., & Gupta, R. (2018). Towards a cyber-physical era: Soft computing framework based multi-sensor array for water quality monitoring. Drinking Water Engineering & Science, 11(1), 1-7. https://doi.org/10.5194/dwes-11-1-2018

Caron, F., Duflos, E., & Pomorski, D. (2017). GPS/IMU data fusion using multi sensor Kalman filtering: Introduction of contextual aspects. Information Fusion, 7(2), 221-230. https://doi.org/10.1016/j.inffus.2009.02.001

Dao, M., Nguyen, N. H., Nasrabadi, N. M., & et al. (2016). Collaborative multi-sensor classification via sparsity-based representation. IEEE Transactions on Signal Processing, 64(9), 2400-2415. https://doi.org/10.1109/TSP.2016.2531028

Erdelj, M., Krol, M., & Natalizio, E. (2017). Wireless sensor networks and multi-UAV systems for natural disaster management. Computer Networks, 124(SEP.), 72-86. https://doi.org/10.1016/j.comnet.2017.05.021

Fantacci, C., & Papi, F. (2016). Scalable multisensor multitarget tracking using the marginalized-GLMB density. IEEE Signal Processing Letters, 23(6), 863-867. https://doi.org/10.1109/LSP.2016.2542739

Fei, Z., Li, B., Yang, S., & et al. (2017). A survey of multi-objective optimization in wireless sensor networks: Metrics, algorithms, and open problems. IEEE Communications Surveys & Tutorials, 19(1), 550-586. https://doi.org/10.1109/COMST.2016.2616340

Janssens, O., Loccufier, M., & Hoecke, S. V. (2019). Thermal imaging and vibration-based multisensor fault detection for rotating machinery. IEEE Transactions on Industrial Informatics, 15(1), 434-444. https://doi.org/10.1109/TII.2018.2869545

Jin, H., Chen, Q., Chen, Z., & et al. (2016). Multi-LeapMotion sensor-based demonstration for robotic refine tabletop object manipulation task. CAAI Transactions on Intelligence Technology, 1(1), 104-113. https://doi.org/10.1109/CIT.2016.22

Muri, H. I., Bano, A., & Hjelme, D. R. (2018). A single point, multi-parameter, fiber optic sensor based on a combination of interferometry and LSPR. Journal of Lightwave Technology, 36(4), 1159-1167. https://doi.org/10.1109/JLT.2017.2780855

Ozger, M., Alagoz, F., & Akan, O. B. (2018). Clustering in multi-channel cognitive radio ad hoc and sensor networks. IEEE Communications Magazine, 56(4), 156-162. https://doi.org/10.1109/MCOM.2018.1700771

Pashko, S. V. (2018). Optimal placement of multi-sensor system for threat detection. Cybernetics & Systems Analysis, 54(2), 249-257. https://doi.org/10.1007/s10559-018-9954-8

Peng, X., Kong, L., Chen, Y., & et al. (2020). Design of a multi-sensor monitoring system for additive manufacturing process. Nanomanufacturing and Metrology, 3(2), 142-150. https://doi.org/10.1007/s41871-020-00055-w

Pokharel, B., Geerts, B., Jing, X., & et al. (2017). A multi-sensor study of the impact of ground-based glaciogenic seeding on clouds and precipitation over mountains in Wyoming. Part II: Seeding impact analysis. Atmospheric Research, 183(JAN.), 42-57. https://doi.org/10.1016/j.atmosres.2016.08.015

Qin, J., Fu, W., Gao, H., & et al. (2017). Distributed k-means algorithm for sensor networks based on multi-agent consensus theory. IEEE Transactions on Cybernetics, 47(3), 772-783. https://doi.org/10.1109/TCYB.2017.2661959

Sobhani, B., Paolini, E., & Giorgetti, A. (2017). Target tracking for UWB multistatic radar sensor networks. IEEE Journal of Selected Topics in Signal Processing, 8(1), 125-136. https://doi.org/10.1109/JSTSP.2017.2666533

Sun, Z., Zhang, Y., Nie, Y., & et al. (2017). CASMOC: A novel complex alliance strategy with multi-objective optimization of coverage in wireless sensor networks. Wireless Networks, 23(4), 1201-1222. https://doi.org/10.1007/s11276-016-1197-1

Verger, A., Baret, F., & Weiss, M. (2016). A multisensor fusion approach to improve LAI time series. Remote Sensing of Environment, 115(10), 2460-2470. https://doi.org/10.1016/j.rse.2011.01.012

Wang, X., Gostar, A. K., Rathnayake, T., & et al. (2018). Centralized multiple-view sensor fusion using labeled multi-Bernoulli filters. Signal Processing, 150(SEP.), 75-84. https://doi.org/10.1016/j.sigpro.2018.04.007

Yan, L., Lu, J., Liu, J., & et al. (2018). Optimal distributed Kalman filtering fusion for multirate multisensor dynamic systems with correlated noise and unreliable measurements. IET Signal Processing, 12(4), 522-531. https://doi.org/10.1049/iet-spr.2017.0231

Yang, X., Zhang, W. A., Yu, L., & et al. (2016). Multi-rate distributed fusion estimation for sensor network-based target tracking. IEEE Sensors Journal, 16(5), 1233-1242. https://doi.org/10.1109/JSEN.2015.2502785

Yu, Z., Chang, L., & Qian, B. (2019). A belief-rule-based model for information fusion with insufficient multi-sensor data and domain knowledge using evolutionary algorithms with operator recommendations. Soft Computing, 23(13), 5129-5142. https://doi.org/10.1007/s00500-018-03407-1

Zeinab, T., Ebtehaj, A. M., & Efi, F. G. (2018). A multi-sensor data-driven methodology for all-sky passive microwave inundation retrieval. Hydrology & Earth System Sciences, 21(6), 2685-2700. https://doi.org/10.5194/hess-21-2685-2017

Zempila, M. M., Fountoulakis, I., & Taylor, M. (2018). Validation of OMI erythemal doses with multi-sensor ground-based measurements in Thessaloniki, Greece. Atmospheric Environment, 183(JUN.), 106-121. https://doi.org/10.1016/j.atmosenv.2018.02.045